Experimental Eye Research 145 (2016) 373–379

Contents lists available at ScienceDirect

Experimental Eye Research

journal homepage: www.elsevier.com/locate/yexer

Axitinib inhibits retinal and choroidal neovascularization in *in vitro* and *in vivo* models

Anand Giddabasappa [a, *], Kush Lalwani [a], Rand Norberg [a], Hovhannes J. Gukasyan [b], David Paterson [a], Ronald A. Schachar [c], Kay Rittenhouse [d], Karen Klamerus [e], Lydia Mosyak [f], Jeetendra Eswaraka [a, **]

[a] Global Science and Technology-WCM, Pfizer Inc., 10724 Science Center Drive, San Diego, CA 92121, USA
[b] Pharmaceutical Sciences, Pfizer Inc., 10724 Science Center Drive, San Diego, CA 92121, USA
[c] Global Clinical Affairs, Pfizer Inc., 10724 Science Center Drive, San Diego, CA 92121, USA
[d] External R&D Innovation, Pfizer Inc., 10724 Science Center Drive, San Diego, CA 92121, USA
[e] Oncology Clinical Development, Pfizer Inc., 10724 Science Center Drive, San Diego, CA 92121, USA
[f] Global Biotherapeutics Technologies, Pfizer Inc., 10724 Science Center Drive, San Diego, CA 92121, USA

ARTICLE INFO

Article history:
Received 15 July 2015
Received in revised form
23 February 2016
Accepted in revised form 25 February 2016
Available online 27 February 2016

Keywords:
Axitinib
Small molecule receptor tyrosine kinase inhibitor
In vitro angiogenesis
3D co-culture model
Rat choroidal neovascularization
Wet age-related macular degeneration

ABSTRACT

Age-related Macular Degeneration (AMD) is the leading cause of visual impairment and blindness in the elderly in developed countries. Neovascular/exudative (wet) AMD is the aggressive form of AMD and can involve choroidal neovascularization and vascular leakage. Anti-vascular endothelial growth factor (anti-VEGF) medications have significantly improved treatment of wet-AMD. However, only approximately 40% of patients obtain full benefit from anti-VEGF therapy and the medications are given by intravitreal injection. Axitinib, a small molecule multi-receptor tyrosine kinase inhibitor used for the treatment of advanced renal cell carcinoma, is taken orally and inhibits VEGF activity by blocking VEGF receptors. Axitinib also has the advantage of blocking platelet derived growth factor (PDGF) receptors which play a role in neovascularization. Using *in vitro* human retinal microvascular endothelial cells (HRMVECs), human brain vascular pericytes (HBVRs), 3D co-culture vessel sprout assay, and *in vivo* laser induced rat choroidal neovascularization (CNV) models, the effect of axitinib on neovascularization was evaluated. Axitinib inhibited neovascularization better than anti-VEGF and/or anti-hPDGF-B mAb in the *in vitro* models demonstrating that combined inhibition of both VEGF and PDGF pathways may be synergistic in treating wet-AMD. Additionally, axitinib showed good efficacy at a low dose (0.875 mg/day) in laser-induced CNV model in rats. In conclusion our data shows that axitinib, an inhibitor of VEGF and PDGF-B pathways may be useful in ameliorating wet-AMD therapy.

Age-related Macular Degeneration (AMD) is the leading cause of visual impairment and blindness in the elderly in developed countries (Ambati and Fowler, 2012; Javitt et al., 2003; Tolentino, 2009). There are two forms of AMD: dry/atrophic AMD and neovascular/exudative (wet) AMD. Dry-AMD affects ~85–90% of AMD patients (Ambati and Fowler, 2012). The hallmark of dry-AMD is the accumulation of drusen and debris in the extracellular space under the retina. Dry-AMD which is the early form can progress to wet-AMD. Wet-AMD affects ~10–15% of AMD patients and is characterized by choroidal neovascularization (CNV) in which new immature blood vessels are formed in the choroid and proliferate towards the outer retina, resulting in inflammation, vascular leakage, retinal edema and visual loss (Ambati and Fowler, 2012; Jager et al., 2008; Zhang et al., 2012).

Neovascularization or angiogenesis involves formation of new blood vessels from mature blood vessels. This is a multi-step process involving proliferation and migration of endothelial cells and pericytes. Neovascularization is orchestrated by a variety of growth factors including vascular endothelial growth factor (VEGF), basic-fibroblast growth factor (bFGF) and platelet derived growth

* Corresponding author. Global Science and Technology (WCM), Pfizer Global Research and Development, 10724 Science Center Dr., San Diego, CA 92121, USA. Tel.: +1 858 622 7522; fax: +1 858 526 4119.
** Corresponding author. Global Science and Technology (WCM), Pfizer Global Research and Development, 10724 Science Center Dr., San Diego, CA 92121, USA.
E-mail addresses: anand.giddabasappa@pfizer.com (A. Giddabasappa), jeetendra.eswaraka@pfizer.com (J. Eswaraka).

http://dx.doi.org/10.1016/j.exer.2016.02.010

factor-B (PDGF-B) (Ahmad et al., 2011; Browning et al., 2008; Dorrell et al., 2007a). Anti-angiogenic drugs targeting VEGF such as Avastin®, Lucentis® and Eylea® (Semeraro et al., 2013; Zhang et al., 2012) are efficacious for treating wet-AMD and other retinal vascular pathologies in patients (Ambati and Fowler, 2012; Tolentino, 2009). Although intravitreal injections of anti-VEGF therapy have significant therapeutic benefit, in some patients visual acuity does not improve or stabilize and some patients become refractory to the therapy over time (Forooghian et al., 2009; Semeraro et al., 2013). As a consequence, new medications alone or in combination with anti-VEGF therapy are being evaluated (Dorrell et al., 2007b; Jo et al., 2006; Mabry et al., 2010a). Pericytes which are regulated through PDGF-B signaling also play an important role in angiogenesis, vascular maturation, stabilization and also resistance to anti-VEGF therapies (Bagley et al., 2005; Benjamin et al., 1998; Jo et al., 2006; Mabry et al., 2010b). Dual targeting of VEGF and PDGF-B signaling pathways have shown synergistic inhibition of angiogenesis in tumor and ocular neovascularization models (Bagley et al., 2005; Jo et al., 2006; Mabry et al., 2010a; Tolentino, 2009) compared to anti-VEGF monotherapy (Zhang et al., 2012). Small molecule kinase inhibitors that target multiple growth factor receptors have been assessed as anti-angiogenic agents in oncology and ocular disease models (Chung et al., 2009; Doukas et al., 2008; Du et al., 2013; Honda et al., 2011; Kang et al., 2013b; Takahashi et al., 2006; Yang et al., 2009).

Axitinib, a multi-receptor tyrosine kinase inhibitor has potent inhibitory effects on VEGFR2, PDGFR-β and KIT receptors. The IC-50 values for VEGFR2, PDGFR-β and KIT were 20 pM, 1.6 nM and 1.7 nM, respectively by receptor phosphorylation assays (Hu-Lowe et al., 2008). The efficacy of axitinib in tumor models is thought to be due to inhibition of tumor angiogenesis (Hu-Lowe et al., 2008; Lu et al., 2015). Pre-clinical studies in various tumor models showed that axitinib (30 mg/kg, twice daily) resulted in 70% tumor growth inhibition (Hu-Lowe et al., 2008). This concentration maintained the efficacious plasma concentration (C_{eff}) for ~12 h with good target inhibition. Currently axitinib (5 mg, twice daily) is approved for use in advanced human renal cell carcinoma. Most common side effects observed at this dose was hypertension (16%), diarrhea (11%) and fatigue (11%) (Gunnarsson et al., 2015). We hypothesize that axitinib can inhibit the retinal and choroidal angiogenesis by blocking both VEGFR and PDGFR-β receptors. In this study we evaluated the efficacy of axitinib using *in vitro* and *in vivo* models of retinal and choroidal neovascularization.

In order to evaluate efficacy of axitinib on retinal angiogenesis *in vitro*, following primary cells of human origin were used: human retinal microvascular endothelial cells (HRMVECs) (CSC systems, Kirkland, WA), human brain vascular pericytes (HBVPs) (ScienCell Research Laboratories, Carlsbad, CA) and human mesenchymal stem cells (hMSCs) (Lonza, Hopkinton, MA). Cells between passage-3 to passage-8 were used in these studies. Both HRMVECs and HBVPs had no significant proliferation under serum free conditions (data not shown). HRMVECs showed a dose dependent proliferative response to human VEGF-165 (hVEGF-165), whereas human PDGF-BB (hPDGF-BB) had no proliferative effect on these cells (data not shown); however, HBVP showed a dose dependent proliferative response to hPDGF-BB, whereas hVEGF-165 had no proliferative effect on these cells (data not shown). These experiments helped us determine 50 ng/ml of growth factor in serum free media as an appropriate condition to evaluate anti-proliferative effects of test compounds.

The IC-50 values of anti-hVEGFA monoclonal antibody (mAb) (a mAb similar to Avastin®), anti-hPDGF-B mAb and axitinib (all agents prepared within Pfizer Inc.) compounds were assessed. Cells in the log phase of growth were plated at 5×10^3 (HRMVEC) and 2.5×10^3 (HBVP) cells/well on a 96 well flat bottom plate and incubated overnight. Then, the plates were washed with serum-free media and incubated with serum-free media containing either hVEGF-165 or hPDGF-BB (R & D Systems, Minneapolis, MN) at 50 ng/ml concentration. Serial dilutions of the compounds to be tested were added in triplicate and incubated for 72 h at 37 °C, in a 5% CO_2 incubator. Viability and proliferation of the cells was quantified with a WST-1 Cell Proliferation assay (absorbance @ 450 nm) (Roche Applied Sciences, Indianapolis, IN) (Chen et al., 2015; Zhang et al., 2015). The effect of test compounds were compared to the proliferation of cells observed at control conditions (serum-free media containing 50 ng/ml of hVEGF-165 or hPDGF-BB). The IC-50 values were determined by non-linear regression analysis using Graph Pad Prizm software (La Jolla, CA). These experiments were repeated at least twice. Fig. 1A and B shows the dose–response curves of anti-hVEGFA mAb, anti-hPDGF-B mAb and axitinib on HRMVECs and HBVPs. There was a dose dependent inhibition of HRMVEC proliferation with IC-50s of 594 pM and 3.72 pM by anti-hVEGFA mAb and axitinib, respectively. Anti-hPDGF-B mAb did not have a significant effect on the proliferation of HRMVECs. In contrast, both anti-hPDGF-B mAb and axitinib dose dependently inhibited the proliferation of HBVPs with IC-50s of 621 pM and 1.79 nM, respectively, but anti-hVEGF mAb did not have any significant effect. These results demonstrated that axitinib inhibits both VEGFR and PDGFR-β mediated angiogenic pathways, albeit with different potency.

Formation of fully differentiated functional blood vessels depends on intimate cell–cell interaction between sprouting endothelial cells, pericytes and/or their progenitor mesenchymal cells. Sprouting endothelial cells secrete PDGF-BB which helps proliferation, differentiation and migration of pericytes to the newly formed endothelial plexus (Benjamin et al., 1998; Darland and D'Amore, 2001). To evaluate co-regulation of retinal endothelial cell and pericyte differentiation, proliferation and new vessel formation, a 3D co-culture sprouting assay (Ding et al., 2004; Hirschi and D'Amore, 1997; Mabry et al., 2010a) was performed. HRMVECs were used to mimic the retinal microenvironment. HRMVECs (5×10^6 cells in EGM2 complete media) were mixed with swollen cytodex-3 micro carrier beads (5000 beads) in flow cytometry tubes. The beads were coated with cells by incubating in a 37 °C incubator for 4 h, accompanied by gentle re-suspension every 15 min. Then the beads and HRMVECs were transferred to a T25 flask with 5 ml EGM2 complete media and incubated overnight at 37 °C. On the second day of the experiment, the HRMVEC-coated beads (50 beads/well) were embedded within a fibrin gel in a 24 well plate. Briefly, human fibrinogen (5 mg/ml) in EGM2 complete media with 0.15 U/ml aprotinin was sterile filtered and HRMVEC-coated beads were suspended. Human mesenchymal cells (hMSCs) at ~4×10^4 per well were suspended in the above fibrinogen media containing HRMVEC coated beads. Thrombin (25 μl of 50 U/ml) was pipetted to the center of each well and 500 μl of fibrinogen + hMSC + HRMVEC-bead suspension was added and gently mixed. After initial incubation at room temperature for 5 min, the plate was incubated for 1 h at 37 °C. Later 1 ml EGM2 complete media was added on top of the gel and incubated for an additional hour at 37 °C. The media on top of the gel was aspirated and 1 ml of 1:1 mixture of EGM2 complete and D551 conditioned media supplemented with 2 ng/ml hHGF (hereafter mentioned as co-culture media) was added. The media was changed every other day with 1 ml of co-culture media for a week. Starting on day 8, the test compounds (anti-hVEGF mAb, anti-hPDGF-B mAb and axitinib) were added with fresh co-culture media. This mixture was replaced every other day until day 15. On day 15 the cells were fixed with 4% paraformaldehyde for 16 h at 4 °C. Each well was washed with PBS-T and incubated with a blocking reagent (10% normal goat serum, 5% BSA, 0.2% Triton X-100 in PBS) for 2 h at room temperature. The

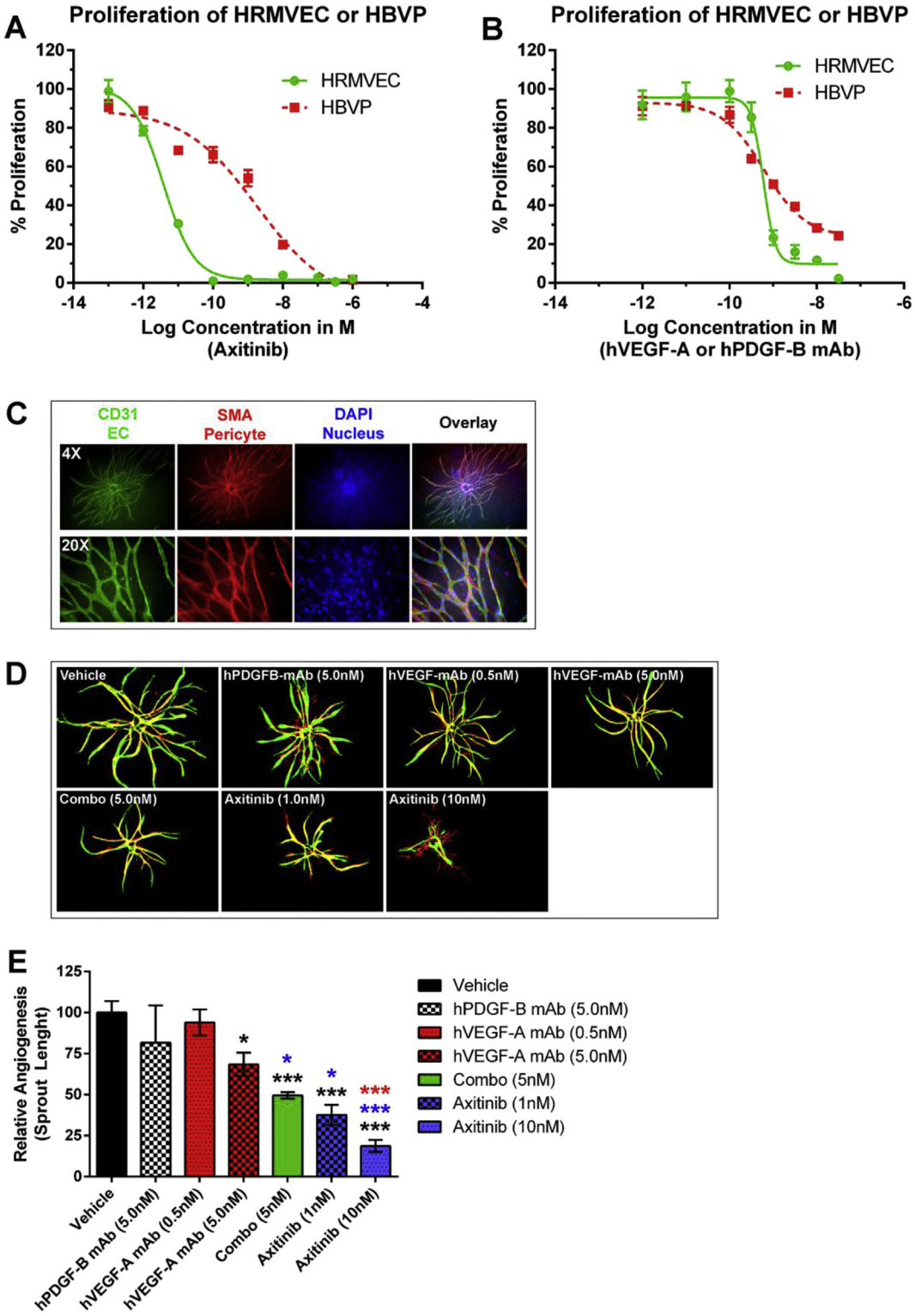

Fig. 1. ***In vitro*** **assays show the superiority of Axitinib compared to anti-VEGF or anti-PDGF-B antibody**. (A) HRMVEC and HBVP proliferation assays show that Axitinib inhibits the proliferation. Axitinib has better sensitivity on HRMVEC compared to HBVP. (B) HRMVEC and HBVP proliferation assays show that anti-hVEGF mAb and anti-hPDGF-B mAb inhibits the proliferation at similar potency. (C) Immunohistochemistry of the Co-culture assay. CD31 was used as an endothelial cell marker; α-SMA was used as a pericyte marker while DAPI was the nucleus marker. The overlay images show (4× and 20×) the co-localization of endothelial cells an pericytes depicting the cell–cell interactions. (D) Schematic images show the effects of anti-hVEGF mAb, anti-hPDGF-B mAb, its combination and axitinib in the co-culture assay. The sprouts in green are endothelial cells and sprouts in red are pericytes had similar architecture. (E) Quantitation of the angiogenic sprouts from co-culture assay show superiority of axitinib compared to other treatments. * in black – vs Vehicle; * in blue – vs anti-hVEGF mAb; * in red – vs Combo of anti-VEGF and anti-PDGF-B mAb. Statistical comparison was performed by Student's t-test. * = $p < 0.05$; ** = $p < 0.005$; *** = $p < 0.0005$.

blocking buffer was replaced with primary antibodies (Rabbit anti-human CD31, Abcam, Cambridge, MA; Mouse anti-human α-smooth muscle actin conjugated to Cy3, Sigma, Saint Louis, MI) and incubated for 48 h at 4 °C. Later the wells were washed with PBS-T and incubated with secondary antibody (Goat anti-rabbit IgG-Alexa Flour 488) and DAPI (Life Technologies Corporation, Grand Island, NY) in the dark for 2 h at room temperature. The wells were rinsed with PBS-T and imaged by fluorescence microscopy. To represent the entire well, 4–6 areas/beads per well were imaged at 4× magnification. The resulting images (in TIFF format) were converted to grayscale image and loaded on to the Image-Pro Plus software (Media Cybernetics Inc, Rockville, MD). Automatic quantitation of tube length was performed using Angiogenesis macro in the Image-Pro Plus software. For each treatment the data is a representative of 4–15 sprouts from 2 separate wells. Student's t-test was performed for statistical comparison between groups.

Immuno-histochemical labeling of the vascular sprouts after the 15 day assay is represented in Fig. 1C. Endothelial cells were labeled with CD31 marker, pericytes with α−SMA and the nucleus with DAPI. An overlay of endothelial cells and pericytes was observed at 20× magnifications at most locations of the sprouts suggesting interdependent growth and similar vascular architecture (Fig. 1C). Fig. 1D shows the representative images of pseudo colored vascular sprouts with endothelial cells (green), pericytes (red) and its overlay (yellow). The quantification of CD31 labeled images is represented in Fig. 1E. Anti-hVEGF mAb showed a dose dependent inhibition of the angiogenic sprouts with ~6% and 32% inhibition at 0.5 nM and 5 nM concentration, respectively (Fig. 1D and E). Although anti-hPDGF-B mAb at 5 nM showed inhibition of angiogenic sprouts, it was statistically not significant compared to the vehicle. Interestingly, a combination of anti-hVEGF and anti-hPDGF-B mAbs at 5 nM concentration synergistically (~53%) inhibited formation of angiogenic sprouts. Axitinib at 1 nM and 10 nM concentration inhibited ~62% and 81% of angiogenic sprouts respectively (Fig. 1D and E). This data confirms that axitinib, which inhibits both VEGFR and PDGFR-β, is superior to either anti-hVEGF and/or anti-hPDGF-B for inhibiting endothelial and pericyte mediated vessel formation.

It was hypothesized that lower doses of axitinib (i.e., <5 mg twice a day approved for use in advanced human renal cell carcinoma) may be able to elicit efficacy while minimizing the tyrosine kinase inhibitor class-related adverse events resulting from systemic concentrations of the drug. To evaluate the effects of low-dose axitinib, a laser induced rat CNV model was used (Edelman and Castro, 2000). All animal experiments were carried out under protocols approved by the Institutional Animal Care and Use Committee (IACUC). Animals were housed under standard 12:12 light:dark cycle in ventilated racks at a room temperature of 72 °F with a relative humidity (RH) between 30 and 70%. Male Brown Norway (BN) rats weighing ~250 g were obtained from Charles River Laboratories, Inc. (Wilmington, MA). The rats were anesthetized with a 1.5 ml/kg intraperitoneal injection of a 1:1 mixture of ketamine HCl (100 mg/ml) dexmedetomidine HCl (0.5 mg/ml). Their eyes were topically anesthetized with 0.5% proparacaine eye drops and their pupils were dilated with 1% tropicamide and 10% phenylephrine HCl topical eye drops for laser photocoagulation and fluorescein angiography. The rats were positioned at a slit lamp with an argon green laser delivery system. Their fundus was visualized using a microscope cover slip with 0.3% hydroxypropyl methylcellulose as an optical coupling agent. Four to six laser photocoagulation spots were created in each eye between major retinal vessels (532 nm wavelength; 110 mW power; 0.1 s duration; and 50 μm spot size; Eyelite 532 nm Ophthalmic Laser; Alcon, Fort Worth, TX). Disruption of Bruch's membrane was confirmed by central bubble formation. Only rats with 4 good lesions in each eye were included in the study. Following laser treatments of both eyes, the animals were randomized into two groups. Each group received axitinib (n = 5) or vehicle (n = 4) 7 days after the laser photocoagulation to follow the interventional treatment paradigm.

Previous pre-clinical and clinical studies showed that axitinib has a very short plasma half-life (~2.5–6.1 h) when dosed orally (Chen et al., 2013; Hu-Lowe et al., 2008; Rixe et al., 2007). Consequently axitinib or its vehicle was administered as a sustained continuous infusion using an osmotic mini pump. Axitinib was formulated in a vehicle composed of 45%DMSO: 40%PEG400: 15% Cremophor ELP mixture and loaded into an Alzet Osmotic Pump - Model 2ML1 (Durect Corporation, Cupertino, CA) according to the manufacturer's instructions. The concentration of axitinib was adjusted to obtain a dose of 0.875 mg/day. For Alzet pump implantation, animals were anesthetized using isoflurane and the surgical site was prepared by clipping the hair followed with ChloraPrep® (San Diego, CA) scrub. Bupivicaine (0.5 mg/kg) was administered subcutaneously at the incision site and an incision was made in the skin. The dosing pump was inserted completely into the pocket with the flow moderator facing away from the incision site and the skin was closed with stainless steel staples. Ketoprofen (5 mg/kg, once daily) was administered 30 min prior to surgery and the next day as an analgesic. At the end of the study, the pumps were removed and evaluated for the release of the drug. Antibodies (anti-hVEGF and anti-hPDGF-B) were not evaluated in this model as they were not rodent reactive.

The effects of axitinib in rat CNV model were evaluated by fluorescein angiography (FA) and isolectin B4 staining. FA is a technique used to assess vascular leakage from the CNV lesions (Edelman and Castro, 2000), whereas isolectin B4 staining is a technique used to evaluate neovascularization (Du et al., 2013). FA was performed on day 14 post-laser photocoagulation as described previously (Edelman and Castro, 2000). Sodium fluorescein (100 mg/kg body weight; AK-Flour 10%, Akron Pharmaceuticals, Lake Forest, IL) was administered intraperitoneally and FA images were captured at 5–10 min after injection. Scoring (0–3 scale) was performed as described in Table 1. The relative number of lesions (as percentage) with FA scores 1–3 is represented in Fig. 2A whereas the mean score of the lesions is represented in Fig. 2B. After FA, the rats were euthanized and eyes were collected for microscopy and image analysis of the choroidal whole mounts. Briefly, eyes were enucleated and stored in 10% formalin for 2 h prior to hemi-section and removal of the lens and neural retina. The resulting eyecups were stained with FITC-conjugated isolectin B4 (Sigma; St. Louis, MO). Then 4–6 radial cuts were made in the eye cups to obtain a flat mount for mounting on a microscope slide (RPE-side facing up) using gel mount media (Aqua-Poly/Mount; Polysciences Inc, Warrington, PA) and a cover slip. CNV lesions were examined using the 10× objective lens of an epifluorescent microscope (Nikon Eclipse; Nikon, Japan) and images were captured using a digital camera attached to the microscope. Representative images are shown in Fig. 2C. The area of CNV lesion was quantified by software Image-Pro Plus 7.0 (MediaCybernetics, Rockville, MD) using a custom designed angiogenesis algorithm. For statistical comparison the mean CNV areas of axitinib group was normalized

Table 1
Fluorescence angiography scoring system.

Score	Definition
0	No leakage
1	Lesions with fluorescence intensity < neighboring major artery or vein
2	Lesions with fluorescence intensity = neighboring major artery or vein
3	Lesions with fluorescence intensity > neighboring major artery or vein

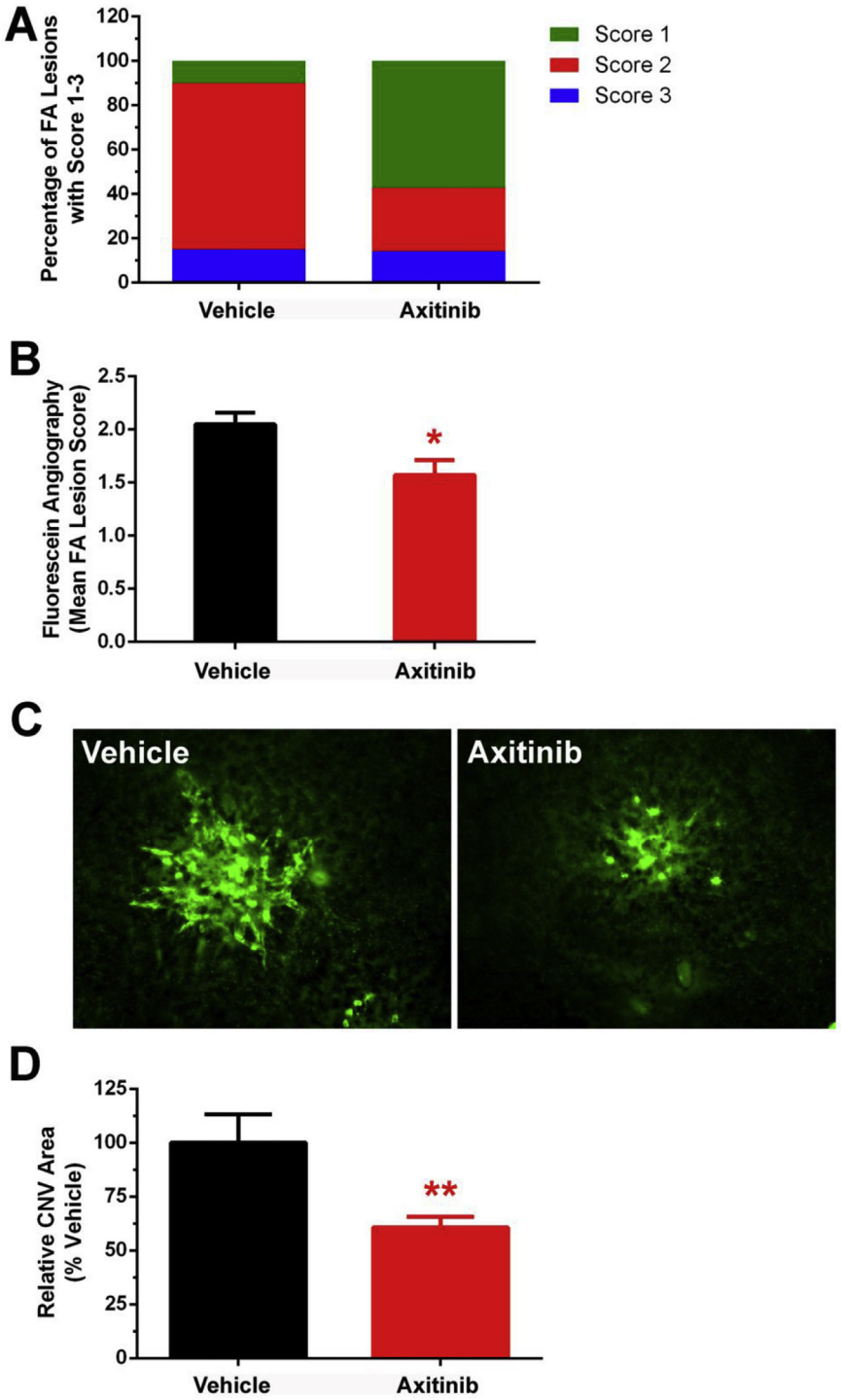

Fig. 2. Axitinib inhibits the angiogenesis and vascular leakage in *in vivo* rat choroidal neovascularization (CNV) model. (A) Fluorescein angiography (FA) shows that axitinib reduces the percentage of lesions with a score equal to 2 (B) and the mean score of the FA lesions in the axitinib treated group is significantly less than the vehicle treated group. (C) Staining of choroidal whole mounts with isolectin B4, a marker of vasculature/endothelial cells show reduction of CNV lesion size. (D) Quantitation of the CNV area using Image-Pro Plus software show statistically significant inhibition of the CNV area in the axitinib treated group compared to the vehicle treated group. Number of lesions scored for FA and CNV was 20–28/group. Statistical comparison was performed by Student's t-test. * = $p < 0.01$; ** = $p < 0.005$.

to day 14 area of the vehicle control group (100%).

FA scoring (as per Table 1), on day 14 post laser photocoagulation showed that ~75% of lesions in the vehicle group had scores equal to 2 (Fig. 2A). The axitinib treated group had maximum lesions with score 1 (~58%) followed by score 2 (~28%) suggesting a dramatic decrease in the score 2 lesions (Fig. 2A). The mean FA score for the vehicle treated eyes was 2.05 (±0.11, SEM) whereas the axitinib treated eyes had a significantly decreased mean FA score of 1.57 (±0.14, SEM) (Fig. 2B) suggesting a decrease in vascular leakage. At the end of the study the eye cups were stained with isolectin B4 and flat mounted for microscopy. A significant reduction (~33% ± 6.7, SEM) in the CNV lesion area was observed in the

microscopic images compared to the vehicle treated group (Fig. 2C and D). These results demonstrated that low dose axitinib was effective in reducing vascular leakage and neovascularization in laser induced CNV rat model.

Anti-VEGF therapy (Lucentis® and Eylea®) has become the standard of care for treating wet-AMD patients (Semeraro et al., 2013; Tolentino, 2009; Zhang et al., 2012). Although this approach has been beneficial to many patients, a significant number of patients do not improve or respond to anti-VEGF therapy because of acquired resistance and/or emergence of alternative pathways for angiogenesis (Jo et al., 2006; Tranos et al., 2013). Angiogenesis involves interaction between multiple cell types. VEGF signaling primarily regulates the proliferation, survival and migration of endothelial cells where as PDGF-BB signaling regulates pericytes. These two cell types interact extensively during angiogenesis (Bagley et al., 2005; Benjamin et al., 1998; Hu-Lowe et al., 2008). Thus inhibiting both cell types may overcome the refractoriness to anti-VEGF monotherapy. There have been a few preclinical and clinical studies showing that the combination of anti-VEGF with anti-PDGFB therapy has additional therapeutic benefit (Jo et al., 2006; Stewart, 2012). The present study, using *in vitro* proliferation assays with HRMVECs and HBVPs demonstrated that anti-VEGF treatment only inhibits endothelial cell proliferation and anti-PDGF-B treatment only inhibits pericyte proliferation, whereas axitinib can inhibit both endothelial and pericyte proliferation. Additionally, axitinib has a 2 log higher sensitivity to VEGFR compared to anti-VEGF mAb, whereas the sensitivity of axitinib to the PDGFR-β was similar to the effect observed with anti-PDGF-B mAb. The 3D sprouting assay is an *in vitro* tool to measure the interaction between endothelial cells and pericyte during the formation of functional vessels. Our results showed that anti-VEGF and anti-PDGF-B mAbs moderately inhibit sprout formation; however, the combination of both anti-VEGF and anti-PDGF-B mAbs and low concentrations of axitinib alone significantly reduced 3D sprout formation. This implies that inhibiting both VEGF and PDGF-B will synergistically reduce neovascularization.

Finally, the tumor growth inhibition studies had demonstrated that 70% anti-tumor efficacy was observed at ~30 mg/kg, twice daily administration (Hu-Lowe et al., 2008). In this study, we show continuous administration of axitinib at a lower dose (0.875 mg/day) for 7 days significantly inhibited vascular leakage and neovascularization in rat CNV model. Consistent with our findings, oral dosing of axitinib at 5 mg/kg inhibited laser induced CNV lesions in a mouse model (Kang et al., 2013a). Additionally, it has been shown that co-administration of axitinib with an anti-VEGF mAb increased the anti-angiogenesis effect of the anti-VEGF mAb (Hu-Lowe et al., 2008). A lower dose of axitinib may reduce its known side effects (Gunnarsson et al., 2015) while still effectively decreasing choroidal neovascularization in wet-AMD patients. Overall, our results show that axitinib, a small molecule inhibitor of VEGF and PDGF-B pathways may be useful in wet-AMD therapy. Future studies evaluating the safety of chronic low-dose axitinib and a sustained release ophthalmic delivery platform may be warranted for its therapeutic utility.

Disclosure of potential conflicts of interest

All authors are either current or former employees of Pfizer.

Acknowledgments

We would like to thank Ken Geles (Pfizer-Oncology Research Unit) for suggestions on *in vitro* co-culture model and Yazdi Pithavala (Pfizer-Oncology Clinical Development) for suggestions on *in vivo* dose selection of Axitinib. The funding for this research and manuscript was provided by Pfizer Inc. All authors are currently or were in past employed by Pfizer Inc.

Appendix A. Supplementary data

Supplementary data related to this article can be found at http://dx.doi.org/10.1016/j.exer.2016.02.010.

References

Ahmad, I., Balasubramanian, S., Del Debbio, C.B., Parameswaran, S., Katz, A.R., Toris, C., Fariss, R.N., 2011. Regulation of ocular angiogenesis by Notch signaling: implications in neovascular age-related macular degeneration. Investig. Ophthalmol. Vis. Sci. 52, 2868–2878.
Ambati, J., Fowler, B.J., 2012. Mechanisms of age-related macular degeneration. Neuron 75, 26–39.
Bagley, R.G., Weber, W., Rouleau, C., Teicher, B.A., 2005. Pericytes and endothelial precursor cells: cellular interactions and contributions to malignancy. Cancer Res. 65, 9741–9750.
Benjamin, L.E., Hemo, I., Keshet, E., 1998. A plasticity window for blood vessel remodelling is defined by pericyte coverage of the preformed endothelial network and is regulated by PDGF-B and VEGF. Development 125, 1591–1598.
Browning, A.C., Dua, H.S., Amoaku, W.M., 2008. The effects of growth factors on the proliferation and in vitro angiogenesis of human macular inner choroidal endothelial cells. Br. J. Ophthalmol. 92, 1003–1008.
Chen, T.C., Tsai, T.Y., Chang, S.W., 2015. Molecular mechanism of fluoroquinolones modulation on corneal fibroblast motility. Exp. Eye Res. 145, 10–16.
Chen, Y., Tortorici, M.A., Garrett, M., Hee, B., Klamerus, K.J., Pithavala, Y.K., 2013. Clinical pharmacology of axitinib. Clin. Pharmacokinet. 52, 713–725.
Chung, E.J., Yoo, S., Lim, H.J., Byeon, S.H., Lee, J.H., Koh, H.J., 2009. Inhibition of choroidal neovascularisation in mice by systemic administration of the multi-kinase inhibitor, sorafenib. Br. J. Ophthalmol. 93, 958–963.
Darland, D.C., D'Amore, P.A., 2001. Cell-cell interactions in vascular development. Curr. Top. Dev. Biol. 52, 107–149.
Ding, R., Darland, D.C., Parmacek, M.S., D'Amore, P.A., 2004. Endothelial-mesenchymal interactions in vitro reveal molecular mechanisms of smooth muscle/pericyte differentiation. Stem Cells Dev. 13, 509–520.
Dorrell, M., Uusitalo-Jarvinen, H., Aguilar, E., Friedlander, M., 2007a. Ocular neovascularization: basic mechanisms and therapeutic advances. Surv. Ophthalmol. 52 (Suppl. 1), S3–S19.
Dorrell, M.I., Aguilar, E., Scheppke, L., Barnett, F.H., Friedlander, M., 2007b. Combination angiostatic therapy completely inhibits ocular and tumor angiogenesis. Proc. Natl. Acad. Sci. U. S. A. 104, 967–972.
Doukas, J., Mahesh, S., Umeda, N., Kachi, S., Akiyama, H., Yokoi, K., Cao, J., Chen, Z., Dellamary, L., Tam, B., Racanelli-Layton, A., Hood, J., Martin, M., Noronha, G., Soll, R., Campochiaro, P.A., 2008. Topical administration of a multi-targeted kinase inhibitor suppresses choroidal neovascularization and retinal edema. J. Cell. Physiol. 216, 29–37.
Du, H., Sun, X., Guma, M., Luo, J., Ouyang, H., Zhang, X., Zeng, J., Quach, J., Nguyen, D.H., Shaw, P.X., Karin, M., Zhang, K., 2013. JNK inhibition reduces apoptosis and neovascularization in a murine model of age-related macular degeneration. Proc. Natl. Acad. Sci. U. S. A. 110, 2377–2382.
Edelman, J.L., Castro, M.R., 2000. Quantitative image analysis of laser-induced choroidal neovascularization in rat. Exp. Eye Res. 71, 523–533.
Forooghian, F., Cukras, C., Meyerle, C.B., Chew, E.Y., Wong, W.T., 2009. Tachyphylaxis after intravitreal bevacizumab for exudative age-related macular degeneration. Retina 29, 723–731.
Gunnarsson, O., Pfanzelter, N.R., Cohen, R.B., Keefe, S.M., 2015. Evaluating the safety and efficacy of axitinib in the treatment of advanced renal cell carcinoma. Cancer Manag. Res. 7, 65–73.
Hirschi, K.K., D'Amore, P.A., 1997. Control of angiogenesis by the pericyte: molecular mechanisms and significance. Exs 79, 419–428.
Honda, M., Asai, T., Umemoto, T., Araki, Y., Oku, N., Tanaka, M., 2011. Suppression of choroidal neovascularization by intravitreal injection of liposomal SU5416. Arch. Ophthalmol. 129, 317–321.
Hu-Lowe, D.D., Zou, H.Y., Grazzini, M.L., Hallin, M.E., Wickman, G.R., Amundson, K., Chen, J.H., Rewolinski, D.A., Yamazaki, S., Wu, E.Y., McTigue, M.A., Murray, B.W., Kania, R.S., O'Connor, P., Shalinsky, D.R., Bender, S.L., 2008. Nonclinical anti-angiogenesis and antitumor activities of axitinib (AG-013736), an oral, potent, and selective inhibitor of vascular endothelial growth factor receptor tyrosine kinases 1, 2, 3. Clin. Cancer Res. Off. J. Am. Assoc. Cancer Res. 14, 7272–7283.
Jager, R.D., Mieler, W.F., Miller, J.W., 2008. Age-related macular degeneration. N. Engl. J. Med. 358, 2606–2617.
Javitt, J.C., Zhou, Z., Maguire, M.G., Fine, S.L., Willke, R.J., 2003. Incidence of exudative age-related macular degeneration among elderly Americans. Ophthalmology 110, 1534–1539.
Jo, N., Mailhos, C., Ju, M., Cheung, E., Bradley, J., Nishijima, K., Robinson, G.S., Adamis, A.P., Shima, D.T., 2006. Inhibition of platelet-derived growth factor B signaling enhances the efficacy of anti-vascular endothelial growth factor therapy in multiple models of ocular neovascularization. Am. J. Pathol. 168, 2036–2053.
Kang, S., Roh, C.R., Cho, W.K., Park, K.C., Yang, K.J., Choi, H.S., Kim, S.H., Roh, Y.J.,

2013a. Antiangiogenic effects of axitinib, an inhibitor of vascular endothelial growth factor receptor tyrosine kinase, on laser-induced choroidal neovascularization in mice. Curr. Eye Res. 38, 119–127.
Kang, S., Roh, Y.J., Kim, I.B., 2013b. Antiangiogenic effects of tivozanib, an oral VEGF receptor tyrosine kinase inhibitor, on experimental choroidal neovascularization in mice. Exp. Eye Res. 112, 125–133.
Lu, L., Saha, D., Martuza, R.L., Rabkin, S.D., Wakimoto, H., 2015. Single agent efficacy of the VEGFR kinase inhibitor axitinib in preclinical models of glioblastoma. J. Neuro Oncol. 121, 91–100.
Mabry, R., Gilbertson, D.G., Frank, A., Vu, T., Ardourel, D., Ostrander, C., Stevens, B., Julien, S., Franke, S., Meengs, B., Brody, J., Presnell, S., Hamacher, N.B., Lantry, M., Wolf, A., Bukowski, T., Rosler, R., Yen, C., Anderson-Haley, M., Brasel, K., Pan, Q., Franklin, H., Thompson, P., Dodds, M., Underwood, S., Peterson, S., Sivakumar, P.V., Snavely, M., 2010a. A dual-targeting PDGFRbeta/VEGF-A molecule assembled from stable antibody fragments demonstrates anti-angiogenic activity in vitro and in vivo. MAbs 2, 20–34.
Mabry, R., Lewis, K.E., Moore, M., McKernan, P.A., Bukowski, T.R., Bontadelli, K., Brender, T., Okada, S., Lum, K., West, J., Kuijper, J.L., Ardourel, D., Franke, S., Lockwood, L., Vu, T., Frank, A., Appleby, M.W., Wolf, A., Reardon, B., Hamacher, N.B., Stevens, B., Lewis, P., Lewis, K.B., Gilbertson, D.G., Lantry, M., Julien, S.H., Ostrander, C., Chan, C., Byrnes-Blake, K., Brody, J., Presnell, S., Meengs, B., Levin, S.D., Snavely, M., 2010b. Engineering of stable bispecific antibodies targeting IL-17A and IL-23. Protein Eng. Des. Sel. 23, 115–127.
Rixe, O., Bukowski, R.M., Michaelson, M.D., Wilding, G., Hudes, G.R., Bolte, O., Motzer, R.J., Bycott, P., Liau, K.F., Freddo, J., Trask, P.C., Kim, S., Rini, B.I., 2007. Axitinib treatment in patients with cytokine-refractory metastatic renal-cell cancer: a phase II study. Lancet Oncol. 8, 975–984.
Semeraro, F., Morescalchi, F., Duse, S., Parmeggiani, F., Gambicorti, E., Costagliola, C., 2013. Aflibercept in wet AMD: specific role and optimal use. Drug Des. Dev. Ther. 7, 711–722.
Stewart, M.W., 2012. Clinical and differential utility of VEGF inhibitors in wet age-related macular degeneration: focus on aflibercept. Clin. Ophthalmol. 6, 1175–1186.
Takahashi, H., Obata, R., Tamaki, Y., 2006. A novel vascular endothelial growth factor receptor 2 inhibitor, SU11248, suppresses choroidal neovascularization in vivo. J. Ocular Pharmacol. Ther. Off. J. Assoc. Ocular Pharmacol. Ther. 22, 213–218.
Tolentino, M.J., 2009. Current molecular understanding and future treatment strategies for pathologic ocular neovascularization. Curr. Mol. Med. 9, 973–981.
Tranos, P., Vacalis, A., Asteriadis, S., Koukoula, S., Vachtsevanos, A., Perganta, G., Georgalas, I., 2013. Resistance to antivascular endothelial growth factor treatment in age-related macular degeneration. Drug Des. Dev. Ther. 7, 485–490.
Yang, X.M., Wang, Y.S., Zhang, J., Li, Y., Xu, J.F., Zhu, J., Zhao, W., Chu, D.K., Wiedemann, P., 2009. Role of PI3K/Akt and MEK/ERK in mediating hypoxia-induced expression of HIF-1alpha and VEGF in laser-induced rat choroidal neovascularization. Investig. Ophthalmol. Vis. Sci. 50, 1873–1879.
Zhang, K., Zhang, L., Weinreb, R.N., 2012. Ophthalmic drug discovery: novel targets and mechanisms for retinal diseases and glaucoma. Nat. Rev. Drug Discov. 11, 541–559.
Zhang, X., Wang, R., Chen, G., Dejean, L., Chen, Q.H., 2015. The effects of curcumin-based compounds on proliferation and cell death in cervical Cancer cells. Anticancer Res. 35, 5293–5298.